Molecular Cancer Therapeutics

Therapeutic Inhibition of the Receptor Tyrosine Kinase AXL Improves Sensitivity to Platinum and Taxane in Ovarian Cancer

Jeanne M. Quinn[1,2], Molly M. Greenwade[1,2], Marguerite L. Palisoul[1,2], Gregory Opara[2], Katina Massad[2], Lei Guo[1,2], Peinan Zhao[1], Hollie Beck-Noia[2], Ian S. Hagemann[3], Andrea R. Hagemann[1], Carolyn K. McCourt[1], Premal H. Thaker[1], Matthew A. Powell[1], David G. Mutch[1], and Katherine C. Fuh[1,2]

Abstract

Ovarian cancer, one of the deadliest malignancies in female cancer patients, is characterized by recurrence and poor response to cytotoxic chemotherapies. Fewer than 30% of patients with resistant disease will respond to additional chemotherapy treatments. This study aims to determine whether and how inhibition of the receptor tyrosine kinase AXL can restore sensitivity to first-line platinum and taxane therapy in ovarian cancer. AXL staining was quantified in a patient tissue microarray and correlated with chemoresponse of patients. We used small hairpin RNAs to knock down AXL expression and the small-molecule inhibitor BGB324 to inhibit AXL and assessed sensitivity of cell lines and primary patient-derived cells to chemotherapy. We quantified platinum accumulation by inductivity-coupled plasma phase mass spectrometry. Finally, we treated chemoresistant patient-derived xenografts with chemotherapy, BGB324, or chemotherapy plus BGB324 and monitored tumor burden. AXL expression was higher in chemoresistant patient tumors and cell lines than in chemosensitive tumors and cell lines. AXL staining significantly predicted chemoresponse. Knockdown and inhibition of AXL dose-dependently improved response to paclitaxel and carboplatin in both cell lines and primary cells. AXL inhibition increased platinum accumulation by 2-fold (*, $P < 0.05$). *In vivo* studies indicated that AXL inhibition enhanced the ability of chemotherapy to prevent tumor growth (****, $P < 0.0001$). AXL contributes to platinum and taxane resistance in ovarian cancer, and inhibition of AXL improves chemoresponse and accumulation of chemotherapy drugs. This study supports continued investigation into AXL as a clinical target.

Introduction

Ovarian cancer is the leading cause of all gynecologic cancer-related deaths worldwide, and high-grade ovarian serous carcinoma is the most common histology. At least 75% of ovarian cancer cases present at the late stages, III and IV, meaning disease has disseminated beyond the ovaries and pelvic organs. Ovarian cancer is initially managed by surgical removal of tumors and then chemotherapy with paclitaxel and carboplatin. However, between 60% and 85% of patients will experience recurrence, and many will develop chemoresistant tumors (1). Of those who develop platinum-resistant disease, fewer than 30% will respond to additional chemotherapy (2). To develop new, effective therapeutic agents will require identification of molecular players in aggressive and chemoresistant ovarian cancer.

One gene of interest in ovarian cancer is the receptor tyrosine kinase AXL. When activated by its only ligand, GAS6, AXL acts through the PI3K/AKT and Ras/ERK pathways to promote proliferation and avoid apoptosis in several tumor types (3–5). AXL is expressed in high-grade ovarian cancers, and AXL overexpression is correlated with poor clinical outcomes. Additionally, in both ovarian cancer and other solid cancers, inhibiting AXL prevents migration and invasion *in vitro* and in mouse models (3, 6–8).

Several lines of evidence indicate that AXL plays a role in chemoresistance. For example, AXL overexpression was demonstrated in lung cancers with acquired resistance to small-molecule inhibitors, such as the EGFR inhibitor erlotinib (9, 10). Two papers showed that inhibiting AXL caused cells to reverse the epithelial-to-mesenchymal transition, which is associated with aggressive and resistant disease features (11, 12). Further, our group demonstrated that inhibiting AXL restored sensitivity to the chemotherapy drug paclitaxel in uterine serous cancer, independent of the epithelial-to-mesenchymal transition (13).

In ovarian cancer, AXL overexpression has been associated with resistance to secondary chemotherapies such as doxorubicin (14). Further, AXL was one of several genes found to be amplified in ovarian cancer cells conditioned in platinum (15, 16). Corno and colleagues demonstrate no significant impact of AXL inhibition on platinum sensitivity in the IGROV-Pt1 cell line (17), while Kanlikilicer and colleagues report a novel AXL inhibitor improves

[1]Division of Gynecologic Oncology, Department of Obstetrics and Gynecology, Washington University School of Medicine, St. Louis, Missouri. [2]Center for Reproductive Health Sciences, Department of Obstetrics and Gynecology, Washington University School of Medicine, St. Louis, Missouri. [3]Department of Pathology and Immunology, Washington University School of Medicine, St. Louis, Missouri.

Note: Supplementary data for this article are available at Molecular Cancer Therapeutics Online (http://mct.aacrjournals.org/).

Corresponding Author: Katherine C. Fuh, Washington University School of Medicine, St. Louis, MO 63110. Phone: 314-362-8155; Fax: 314-362-2893; E-mail: kfuh@wustl.edu

doi: 10.1158/1535-7163.MCT-18-0537

©2018 American Association for Cancer Research.

Downloaded from http://aacrjournals.org/mct/article-pdf/18/2/389/1861208/389.pdf by guest on 31 March 2023

response to paclitaxel, but only in an intraperitoneal mouse model and without mechanistic investigation (8). However, no work has yet addressed whether or not AXL expression contributes to ovarian cancer resistance to the standard-of-care treatments paclitaxel and carboplatin and a mechanism by which this occurs. We addressed this question here and report that AXL is overexpressed in chemoresistant ovarian cancer tumors and that inhibiting AXL improves response to paclitaxel and carboplatin. These results suggest that targeting AXL might provide new strategies for treating chemoresistant ovarian cancer.

Materials and Methods

Human tissue microarrays and IHC

A tissue microarray containing specimens from primary and metastatic ovarian cancer tumors collected during debulking surgeries was constructed under Institutional Review Board (IRB) approval #201709191 in accordance with recognized ethical guidelines per the U.S. Common Rule. Patients were treated at Washington University in St. Louis, and informed written consent was obtained for tissue banking. Cases were considered chemoresistant if disease recurred within 6 months after adjuvant chemotherapy was completed. Deparaffinized and rehydrated microarray slides were stained with an anti-AXL primary antibody (R&D Systems), and two sections were analyzed per tumor. Intensity and quantity of positive staining was scored blindly, averaged, stratified, and assigned a histology score (h-score; 0 for 0%–20%, 1 for 21%–50%, 2 for 51%–75%, and 3 for 76%–100%), as developed and validated by Rankin and colleagues (18). We assigned scores 0 and 1 as "low AXL," and scores 2 and 3 as "high AXL."

Cell lines

Previously established metastatic ovarian cancer cell lines were cultured in RPMI (Sigma-Aldrich) supplemented with 10% heat-inactivated fetal bovine serum (Sigma-Aldrich) and 1% penicillin and streptomycin (Thermo Fisher; ref. 19). OVCAR3 and OVCAR3TP cells were obtained from B. Sikic (20) in 2014; OVCAR4 and OVCAR5 cells were obtained from NCI in 2015; and OVCAR8 cells were obtained from E. Rankin in 2009 (18). OVCAT3TPMES cells were isolated from mouse mesentery tumor nodules in an OVCAR3TP intraperitoneal model. Primary ovarian high-grade serous carcinoma cells (POV) were isolated from patient ascites collected with informed written consent, and cultured in DMEM (Sigma-Aldrich) supplemented with 20% fetal bovine serum and 1% penicillin and streptomycin. All cells were maintained at 37°C in a 5% CO_2 incubator. Cell lines were authenticated by IDEXX Bioresearch. All cell lines were confirmed negative for *Mycoplasma*, as indicated by the MycoAlert Mycoplasma Detection Kit (Lonza).

Western blot analysis

Protein lysates were collected in 9 mol/L urea, 0.075 mol/L Tris, pH 7.6, and were quantified with the Bradford assay. Lysates were subjected to reducing SDS-PAGE and transferred to nitrocellulose membrane by standard methods. Western blots were probed with antibodies against AXL (1:1,000, R&D Systems), β-actin (1:1,000, Sigma-Aldrich), p-AXL702/703 (1:500, Cell Signaling), GAS6 (1:1,000, R&D Systems), pSRC (1:500, Cell Signaling), and SRC (1:1,000, Cell Signaling). Corresponding horseradish peroxidase-conjugated secondary antibodies (Jackson ImmunoResearch) and the ECL kit were used (Thermo Fisher), and chemiluminescence was measured on a ChemiDoc (Bio-Rad Laboratories).

Drug treatment and cell growth (XTT) assays

The day before drug treatment, 5×10^3 cells were plated in each well of a 96-well plate and allowed to attach overnight. Then, cells were treated with 0.7 nmol/L to 320 nmol/L paclitaxel (Sigma-Aldrich) or 2.8 μmol/L to 1,280 μmol/L carboplatin (Teva Pharmaceuticals). Cells were pretreated with the AXL small-molecule inhibitor BGB324 (also known as R428 or bemcentinib; Selleckchem; ref. 21) for 4 hours and were then treated with a combination of chemotherapy and BGB324. After 72 hours, a 2,3-bis(2-methoxy-4-nitro-5-sulfophenyl)-2H-tetrazolium-5-carboxanilide inner salt (XTT)-based assay (Sigma-Aldrich) was performed as previously described to measure viability (22). The 96-well plates were returned to the 37°C incubator for 2 to 4 hours. Metabolism of XTT was quantified by measuring the absorbance at 450 nm (Tecan infinite M200 Pro). Experimental data were quantified relative to values obtained for cells treated with vehicle only.

Stable transfection with short hairpin RNA

Oligos encoding AXL shRNAs were synthesized as previously described (13) and cloned into the pSiren RetroQ vector (BD Biosciences). Viral particles were produced in 293T cells, and target cells were incubated with viral media for 24 hours. The immortalized cell line POV71-hTERT was created by infecting POVs with viruses made containing the pBABE-hygro-hTERT plasmid (23). Cells were selected in puromycin (Sigma-Aldrich) or hygromycin B (Thermo Fisher), and AXL knockdown was validated by Western blot.

cDNA preparation and quantitative real-time PCR

The RNAEasy plus mini kit (Qiagen) was used to isolate total cellular RNA, 1 μg of which was used to make cDNA by using the SuperScript IV system (Thermo Fisher) according to the manufacturer's directions. An Applied Biosystems 7500 detection system and SYBR-green master mix (Thermo Fisher) were used to perform quantitative RT-PCR. mRNA expression was normalized with respect to glyceraldehyde-3-phosphate dehydrogenase, and fold change was calculated by the $2^{(-\Delta\Delta CT)}$ method. Primer sequences were previously published (18, 24–26).

Measuring platinum accumulation

Cells were pretreated with various doses of BGB324 for 2 hours, then cotreated with BGB324 and 100 μmol/L carboplatin. A validated inductivity-coupled plasma mass spectroscopy (ICP-MS) method (27) was used to measure platinum concentration in lysates from carboplatin-treated cells. Briefly, samples were digested in concentrated HNO_3 for 40 minutes at 200°C by using the Mars 6 microwave digestion system (CEM), then diluted in deionized water to 3.5% HNO_3. Platinum content was measured with a NexION2000 ICP-MS (PerkinElmer) and corresponding software (Agilent MassHunter). Apparent platinum concentration was standardized to total protein and reported as ng platinum/mg protein.

RNA sequencing of patient tumors

Patient samples were obtained during laparoscopic biopsies under protocol #201401756, and after written, informed written consent was obtained. Follow-up time was 31 to 38 months after

Downloaded from http://aacrjournals.org/mct/article-pdf/18/2/389/1861208/389.pdf by guest on 31 March 2023

Table 1. Disease characteristics and chemoresponse in human ovarian cancer

Chemoresponse	Chemoresistant ($n = 27$)	Chemosensitive ($n = 37$)	No recurrence ($n = 35$)	Total ($N = 99$)
Stage				
I	0 (0%)	3 (15%)	17 (85%)	20
II	1 (20%)	1 (20%)	3 (60%)	5
III	23 (33%)	31 (45%)	15 (22%)	69
IV	3 (60%)	2 (40%)	0 (0%)	5
Grade				
1	0 (0%)	0 (0%)	5 (100%)	5
2	1 (7%)	6 (43%)	7 (50%)	14
3	26 (33%)	31 (39%)	22 (28%)	79
Mixed	0 (0%)	0 (0%)	1 (100%)	1
Histology				
High-grade serous	26 (34%)	33 (43%)	17 (22%)	76
Low-grade serous	0 (0%)	0 (0%)	0 (0%)	0
Endometrioid	0 (0%)	2 (18%)	9 (82%)	11
Clear cell	1 (13%)	1 (13%)	6 (75%)	8
Mixed	0 (0%)	1 (25%)	3 (75%)	4
Tumor AXL staining				
3	41%	39%	20%	
2	44%	37%	19%	
1	18%	51%	31%	
0	0%	36%	64%	
Mean H-score	2.3	1.9**	1.6***	

NOTE: The asterisk indicates significant difference in AXL histology score from chemoresistant (**, $P = 0.0045$; ***, $P = 0.001$).

diagnosis and 24 to 33 months after completing initial chemotherapy. Tumor samples were frozen, lysed, and subjected to RNA sequencing. Manual libraries (single indexes) were constructed by using the Illumina TruSeq Stranded total RNA kit (Illumina; 100–500 ng of total RNA) according to the manufacturer's instructions. KAPA qPCR was used to quantify the libraries and determine the appropriate concentration to produce optimal recommended cluster density on a HiSeq4000 v2 (PE150bp) sequencing run. All sequencing runs were completed according to the manufacturer's recommendations (Illumina Inc.).

Patient-derived xenograft model

Female NSG (NOD.Cg-Prkdcscid Il2rgtm1Wjl/SzJ) mice (Jackson Laboratories) ages 7 to 8 weeks were used for tumor xenograft experiments, according to institutional animal care and use policy (IACUC, #20170203) and IRB protocol #201105400. Patient-derived tumors were implanted subcutaneously onto the flank until tumor engraftment and growth were observed. Xenografts were then expanded and passaged into mice for drug treatment experiments. Therapy was administered at dosages of 20 mg/kg paclitaxel, 90 mg/kg carboplatin, and 14 mg/kg BGB324. Chemotherapy was delivered twice weekly by intraperitoneal injection, and BGB324 was delivered daily by oral gavage. Tumors were measured every 3 days with calipers, and tumor volume was calculated with the equation $V = l * w * \pi/6$ (l = longest diameter, w = shortest, perpendicular diameter). Relative tumor volume for control and treatment conditions (V_C or V_T) were calculated by normalizing tumor volume at day 31 or experimental endpoint over tumor volume at day 1. Relative tumor growth (V_T/V_C) was then calculated for each treatment condition.

Statistical analyses

GraphPad Prism 7 was used for statistical analyses and IC_{50} calculations. Statistical significance of differences between groups was determined by two-tailed unpaired t tests or one-way ANOVA and defined as $P < 0.05$. AXL staining in patient tissue and clinical outcomes were analyzed by Kaplan–Meier regression, and significance was determined by log-rank tests. χ^2 tests were performed on low (0%–70%) or high (71%–100%) AXL expression in tumors, as separated by median % AXL staining. Multivariate analyses for chemoresistance using a Cox proportional model and log-rank tests were performed on AXL expression level, disease stage, disease grade, patient age, and debulking status to determine whether AXL independently associated with rates of chemoresistance. Multivariate logistic regression was performed to determine whether AXL expression could be used to predict chemoresponse. These statistical analyses were performed with SAS (version 9.4, SAS Institution Inc.).

Results

AXL is upregulated in chemoresistant ovarian cancer patient tumors

To confirm and extend reports that AXL is overexpressed in ovarian cancer tumors (18), we performed IHC analysis on human tissue microarrays containing primary and metastatic tumors from patients treated at Washington University (St. Louis, MO). A summary of clinical characteristics from the ovarian cancer cases included in the tissue microarrays can be found in Table 1. We used Kaplan–Meier regression analysis to compare the overall survival of patients with tumors expressing low versus high levels of AXL (Supplementary Fig. S1A). Consistent with previous findings (1), patients with low AXL had a median overall survival of 99 months, whereas patients with high AXL had a significantly shorter median overall survival of 35.7 months (**, $P = 0.007$). We also assessed progression-free survival in these groups and found that patients with high AXL recurred more quickly (11.3 months) than patients with low AXL (23.9 months; **, $P = 0.005$; Supplementary Fig. S1B).

Given our previous findings that high AXL levels correlated with chemoresistance in endometrial cancer patients (13), we investigated the correlation between AXL level and chemoresponse in 170 ovarian cancer tumors (Fig. 1A). We found that

Downloaded from http://aacrjournals.org/mct/article-pdf/18/2/389/1861208/389.pdf by guest on 31 March 2023

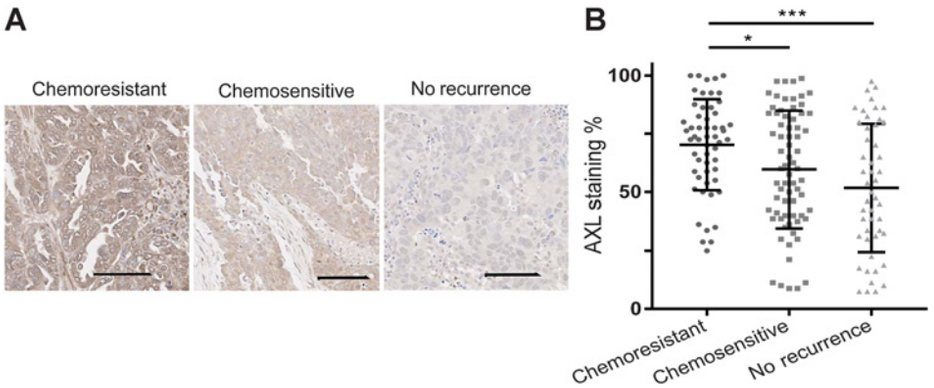

Figure 1.
AXL is amplified in chemoresistant ovarian cancer. **A,** Representative images of AXL staining in ovarian cancer tumors grouped by patient chemoresponse. Scale bar, 100 μm. **B,** Percent AXL staining in chemoresistant, chemosensitive with recurrence, or chemosensitive with no recurrence tumors. Error bars, mean and interquartile range. *, $P < 0.05$; ***, $P < 0.001$.

chemoresistant tumors expressed higher AXL than chemosensitive or nonrecurrent tumors (*, $P < 0.05$; ***, $P < 0.001$, respectively; Fig. 1B; Supplementary Table S1). Further, multivariate analysis was performed to assess the contribution of disease stage, grade, debulking status, age, and AXL expression to the development of chemoresistance (Supplementary Table S2). Disease grade, debulking status, and AXL expression were all significant independent factors in predicting chemoresponse (**, $P = 0.0096$; **, $P = 0.0019$; *, $P = 0.0177$, respectively). The fit model was found to have 74.8% accuracy.

High AXL level is associated with ovarian cancer resistance to paclitaxel and carboplatin

To determine whether AXL level correlated with response to chemotherapy in ovarian cancer, we first screened five ovarian cancer cell lines for AXL expression. We did not detect AXL in OVCAR3 cells but did detect AXL and phosphorylated AXL in OVCAR3TP, OVCAR3TPMES, OVCAR5, and OVCAR8 metastatic cell lines (Fig. 2A). We found that the AXL-null line OVCAR3 was significantly more sensitive to both paclitaxel and carboplatin than the AXL-expressing cell lines (Fig. 2B and C).

Genetic inhibition of AXL increases ovarian cancer sensitivity to paclitaxel and carboplatin

To determine whether AXL expression contributed to chemoresistance, we used lentiviruses to deliver an AXL-specific short hairpin RNA construct (shAXL-S) or scrambled sequence (shSCRM) to OVCAR3TPMES and OVCAR5 cells. Because this shRNA did not completely eliminate AXL expression (Fig. 2D), we transfected parental OVCAR5 cells with three additional AXL-targeting shRNAs (shAXL-C4, shAXL-D3, or shAXL-D4; Fig. 2E). We then treated these cells with vehicle or increasing concentrations of chemotherapy for 72 hours and assessed viability via the XTT assay and found that AXL depletion increased sensitivity to both paclitaxel and carboplatin (Fig. 2F and G).

Inhibiting AXL with BGB324 improves response to paclitaxel and carboplatin in ovarian cancer cell lines

Next, we examined the effects of inhibiting AXL with the small-molecule inhibitor BGB324 (bemcentinib, R428; ref. 21). The OVCAR5, OVCAR3TP, and OVCAR3TPMES cell lines were pretreated with BGB324 for 4 hours and were then exposed to increasing concentrations of paclitaxel or carboplatin for 72 hours. Treatment with 0.25 μmol/L BGB324 was able to suppress pAXL and downstream pSRC detection in the context of GAS6 stimulation, consistent with previous findings (Supplementary Fig. S2; ref. 13). In all cell lines, BGB324 improved responses to paclitaxel and carboplatin in a dose-dependent manner (Table 2). For example, cotreatment with 1 μmol/L BGB324 reduced carboplatin IC_{50} values by 1.66- to 2.38-fold and reduced paclitaxel IC_{50} values by 1.57- to 2.51-fold (*, $P < 0.05$). We previously reported that BGB324 alone at these concentrations had no significant effect on cell viability (13). Additionally, others have reported that BGB324 did not affect invasion, migration, or chemoresponse of AXL-deficient cells (11). Collectively, these data demonstrate that inhibiting AXL improves ovarian cancer sensitivity to carboplatin and paclitaxel.

Inhibiting AXL increases sensitivity to paclitaxel and carboplatin in primary ovarian cancer cells

Given these findings, we wondered if similar therapeutic AXL inhibition could restore chemosensitivity in human primary ovarian cancer. Although ovarian cancer cell lines were qualitatively referred to as more or less chemoresistant, we utilized the tumor cells from a patient with known chemoresistance (Supplementary Table S3) to validate the efficacy of AXL inhibition. IHC of a metastatic tumor from this patient revealed that the tumor expressed a high level of AXL (h-score = 3; Fig. 3A). We cultured patient ascites until ovarian cancer cells proliferated and could be passaged, and then transfected them with the lentiviral plasmid hTERT-hygro-pBABE to immortalize the primary cells. We pretreated these POV71-hTERT cells with 1 or 2 μmol/L BGB324 or vehicle for 4 hours, cotreated them with BGB324 plus paclitaxel or carboplatin for 72 hours, and then assessed relative viability via the XTT assay (Fig. 3B and C). We found that 1 and 2 μmol/L BGB324 reduced the paclitaxel IC_{50} by 1.90- and 1.93-fold, respectively, and that 1 and 2 μmol/L BGB324 reduced the carboplatin IC_{50} by 1.21- and 2.43-fold, respectively. Although cotreatment IC_{50} values were still higher than cell line IC_{50} values, this may be because of how chemoresistant the patient tumor was initially, or because these immortalized primary cells proliferate much quicker than standard cell lines, necessitating larger doses of antimitotic chemotherapies. Taken together, these results indicate that inhibiting AXL with BGB324 increases chemosensitivity in primary cells derived from a chemoresistant patient tumor.

Downloaded from http://aacrjournals.org/mct/article-pdf/18/2/389/1861208/389.pdf by guest on 31 March 2023

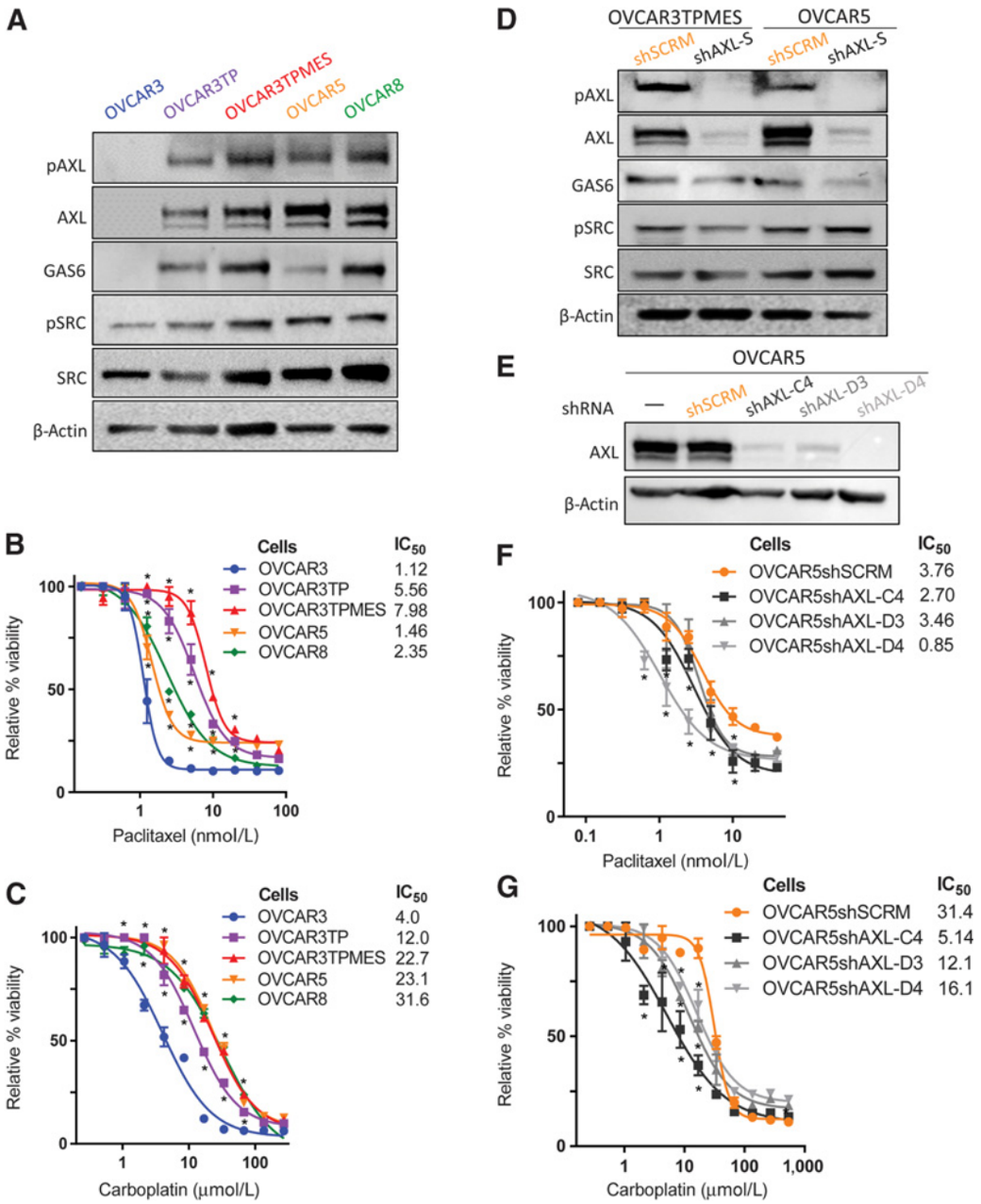

Figure 2.

AXL expression is elevated in ovarian cancer cell lines resistant to paclitaxel and carboplatin, and genetic inhibition of AXL improves chemosensitivity. **A,** Western blot detection of AXL in OVCAR3, OVCAR3TP, OVCAR3TPMES, OVCAR5, and OVCAR8 cells with β-actin used as a loading control. **B** and **C,** Results of the XTT assay of cell viability in increasing concentrations of paclitaxel (**B**) or carboplatin (**C**). XTT assays were performed in triplicate and are graphed as the mean ± SD. *, $P < 0.05$ compared with AXL-null OVCAR3. **D,** Western blot of AXL detection in OVCAR3TPMES and OVCAR5 cells transfected with shAXL or shSCRM control. **E,** Western blot detection of AXL in OVCAR5 cells transfected with shSCRM control or AXL-targeting shSCRM-C4, shSCRM-D3, or shAXL-D4. **F** and **G,** Results of the XTT assay of cell viability in increasing concentrations of paclitaxel (**F**) or carboplatin (**G**). Cell viability is expressed relative to the respective controls treated with vehicle. Assays were performed in triplicate and are graphed as the mean ± SD. *, $P < 0.05$ compared with matched shSCRM controls.

AXL inhibition affects carboplatin accumulation and gene expression in primary ovarian cancer cells

We previously showed that uterine serous cancer cells treated with BGB324 accumulated more paclitaxel than did cells without inhibitor treatment (13). To determine whether AXL similarly affected chemotherapy accumulation in ovarian cancer cells, we treated POV71-hTERT with BGB324 for 2 hours, then added carboplatin for an additional 2 hours. We then quantitated intracellular carboplatin and found that cells treated with 1 or 2 μmol/L BGB324 contained 2.05- or 1.92-fold

Downloaded from http://aacrjournals.org/mct/article-pdf/18/2/389/1861208/389.pdf by guest on 31 March 2023

Table 2. AXL inhibition by BGB324 restores chemosensitivity in OvCa cell lines

		Chemotherapy IC_{50} at indicated BGB324 doses (μmol/L)			
Cell line	**Chemotherapy**	**0**	**0.25**	**0.5**	**1**
OVCAR5	Carboplatin (μmol/L)	80.5	80.1	55.5**	36.4***
	Paclitaxel (nmol/L)	8.4	5.1**	4.6**	4.2***
OVCAR3TP	Carboplatin (μmol/L)	67.7	60.9	44.2**	40.9*
	Paclitaxel (nmol/L)	17.1	12.2*	8.5***	6.8**
OVCAR3TPMES	Carboplatin (μmol/L)	73.0	66.2	50.7**	30.6**
	Paclitaxel (nmol/L)	15.4	13.0	11.3*	9.8*

NOTE: *, $P < 0.05$; **, $P < 0.01$; ***, $P < 0.005$ compared with DMSO control.

more platinum, respectively, than untreated cells (*, $P < 0.05$; **, $P < 0.01$; Fig. 3D). This finding suggests that AXL inhibition improves response to chemotherapy by increasing accumulation of drug.

In an attempt to determine the mechanism by which BGB324 increased response to chemotherapy, we examined gene expression in POV71-hTERT cells by quantitative RT-PCR. Because mesenchymal cells are more resistant to chemotherapy than epithelial cells (9, 11, 25, 28, 29), we examined expression of the epithelial-to-mesenchymal transition genes CDH1 (encoding E-cadherin) and SNAIL. Expression of CDH1 was significantly higher in cells treated with BGB324 for 72 hours than in untreated cells. Expression of SNAIL was lower, but this trend was not statistically significant (Fig. 3E). We next examined expression of the multidrug resistance gene PGP and found that, as reported for other cancer types (13, 30), BGB324-treated cells expressed significantly less PGP than untreated cells (Fig. 3E). Similarly, they expressed less of the ABC transporter ABCC3 (MRP3), but this difference was not statistically significant. Sustained AXL inhibition has been shown to reverse mesenchymal phenotype markers, reducing cross-activation and leading to a shift in lower AXL transcripts (31). We believe that this AXL inhibition may be accompanied by reduction in MDR protein transcription and activity. Accordingly, we noted that AXL expression was significantly lower in BGB324-treated cells than in untreated cells.

To assess the broader relevance of the connection between AXL expression and expression of multidrug resistance genes, we performed RNA sequencing on tumor biopsies taken from 6 patients before they began therapy (Supplementary Table S3). *t* tests were performed to compare transcript levels between groups of patients from two main categories: (i) patients whose tumors recurred and were alive with disease or died of disease (AWD/DOD), and (ii) patients whose tumors never recurred and had no evidence of disease after chemotherapy (NED; Fig. 3F). Tumors from patients in the AWD/DOD group had more AXL transcripts than tumors from patients in the NED group (Fig. 3F). Analysis of transcript levels from 80 genes related to chemoresponse revealed two multidrug resistance genes that were significantly more highly expressed in tumors from the AWD/DOD group than in tumors from the NED group (Fig. 3F). Conversely, no transcripts corresponding to resistance proteins were found to be higher in the NED group. We found that ABCA3 and ABCB9 transcripts were upregulated in the poor responders, and these transporters are specifically related to platinum and taxane accumulation (32–34). Taken together, these accumulation and transcript data suggest that AXL expression is associated with markers of chemoresistance.

AXL inhibition maintains response to chemotherapy in a patient-derived xenograft model

Finally, we sought to determine the effect of inhibiting AXL on ovarian cancer growth *in vivo*. Thus, we used a patient-derived xenograft (PDX) model from a chemoresistant tumor (PB1; Supplementary Table S3). We confirmed by IHC that the tumor expressed AXL (Fig. 4A). We then engrafted PB1 in mice and treated with vehicle, BGB324, paclitaxel plus carboplatin, or paclitaxel plus carboplatin followed by BGB324. Although BGB324 alone had no effect on tumor growth, tumors grew significantly less in mice treated with chemotherapy followed by BGB324 than in any of the other three groups (****, $P < 0.0001$; Fig. 4B).

To examine gene expression in the tumors, we resected these at day 31 from mice treated with vehicle, day 34 for mice treated with BGB324 alone, and day 64 from mice treated with paclitaxel plus carboplatin or paclitaxel and carboplatin followed by BGB324. With limited tumor from the chemotherapy followed by the BGB324 group, we assessed transcriptional differences rather than differences of protein expression. By qRT-PCR analysis, we found that tumors from mice treated with paclitaxel plus carboplatin had significantly amplified AXL transcripts than did tumors from mice treated with vehicle, BGB324 alone, or BGB324 plus paclitaxel and carboplatin (Fig. 4C). This finding is reminiscent of the report by Oien and colleagues that continued cisplatin treatment in mesothelioma cells can increase AXL expression and that BGB324 treatment can prevent this effect (35).

At day 31, tumor proliferation rates in mice treated with paclitaxel and carboplatin were significantly reduced than tumors from mice treated with vehicle or BGB324 (****, $P < 0.001$; Fig. 4D). By day 64, tumors from mice treated with paclitaxel and carboplatin were proliferating at a significantly higher rate than tumors from mice treated with paclitaxel and carboplatin followed by BGB324 (**, $P < 0.01$; Fig. 4E). This aligns with our findings that chemotherapy alone is not able to sustain its therapeutic efficacy in ovarian cancer. Interestingly, administration of BGB324 after chemotherapy was able to maintain the low tumor volume even after BGB324 treatment had ended. Overall, tumor growth was most inhibited only when both chemotherapy and BGB324 were administered, and AXL amplification was prevented (****, $P < 0.001$). These results indicate that AXL inhibition contributes to the *in vivo* sensitivity of patient-derived ovarian cancer xenografts to chemotherapy.

Discussion

Despite effectiveness of the first-line carboplatin and paclitaxel regimen, the majority of ovarian cancer patients die because they develop chemoresistant disease (36, 37). Numerous receptors and pathways are known to be critical in ovarian cancer

Downloaded from http://aacrjournals.org/mct/article-pdf/18/2/389/1861208/389.pdf by guest on 31 March 2023

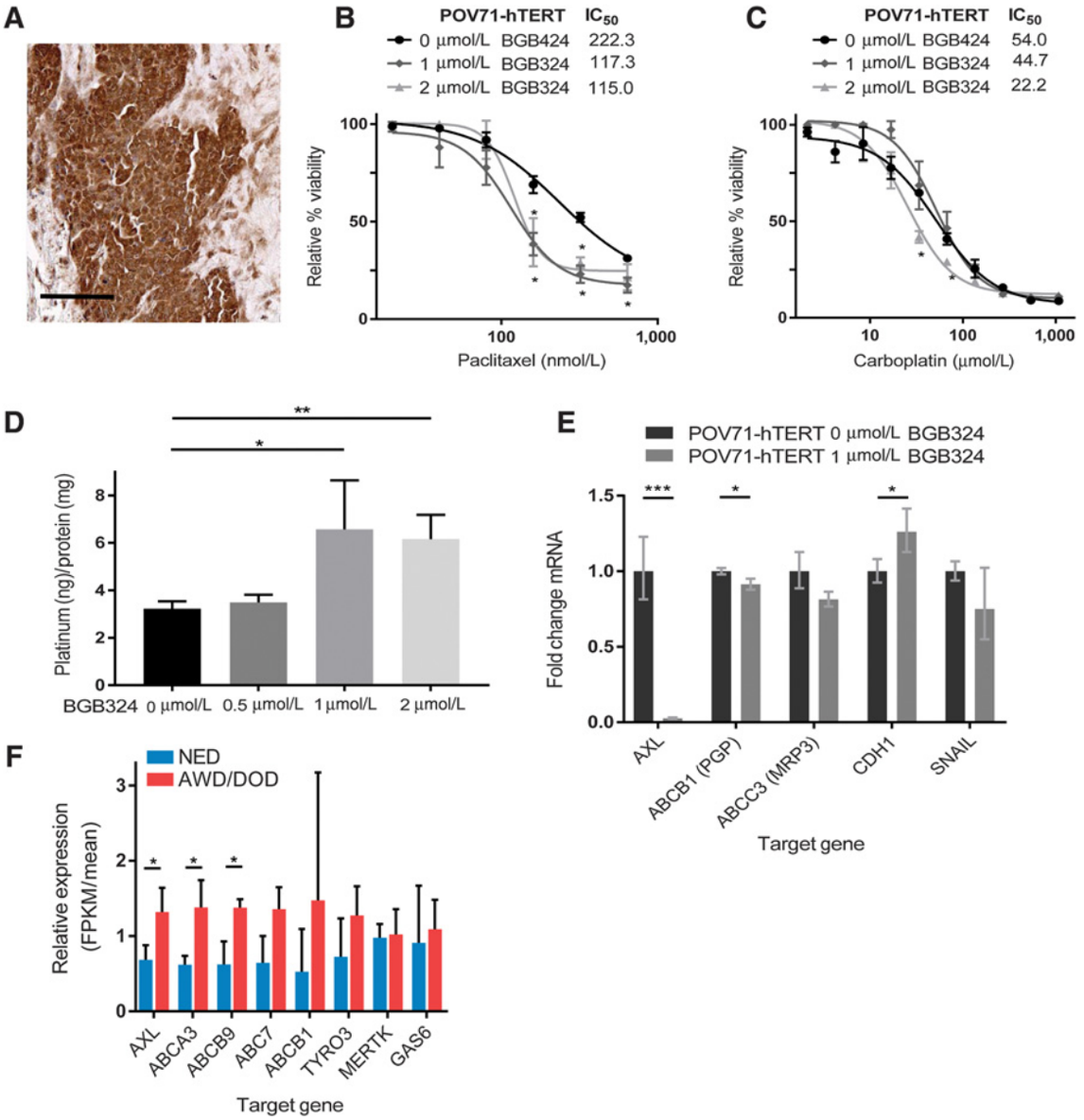

Figure 3.

Therapeutic inhibition of AXL affects chemoresponse and gene expression in primary ovarian cancer cells. **A,** Results of IHC against AXL in a metastasis from patient 71. Scale bar, 100 µm. **B** and **C,** Cell viability as measured by the XTT assay when pretreated with the indicated doses of BGB324 and increasing concentrations of paclitaxel (**B**) or carboplatin (**C**). Cell viability is expressed relative to the respective controls treated with vehicle. XTT assays were performed in triplicate and are graphed as the mean ± SD. *, $P < 0.05$ compared with matched controls. **D,** Quantitation of intracellular platinum in cells treated with vehicle or BGB324, followed by treatment with carboplatin. **E,** qPCR was performed on primary cells treated with BGB324 and expression patterns of mRNA were assessed. Error bars, range of the fold change, and significance was calculated using SD of DDC_T. *, $P < 0.05$. **F,** Relative difference in FPKM levels constructed from RNA-sequencing patient tumor transcript levels. *, $P < 0.05$; **, $P < 0.01$; ***, $P < 0.001$.

chemoresistance (38–51), but no targeted agent has been shown to enhance sensitivity to both carboplatin and paclitaxel. Here, we present several lines of evidence that AXL has a critical role in resistance to paclitaxel and carboplatin. First, we demonstrate that chemoresistant ovarian cancer tumors have significantly higher AXL protein expression than chemosensitive tumors. Second, we establish, for the first time in any cancer, that high AXL expression predicts chemoresistance in patient tumors. Third, we show that high AXL mRNA expression in pretreatment tumors correlates with disease burden. Fourth, we demonstrate that inhibiting AXL with BGB324 improves primary ovarian cancer response to carboplatin and paclitaxel. Our data suggest that this may occur via enhanced platinum accumulation. Finally, we show that the combination of BGB324 with paclitaxel and carboplatin significantly decreases tumor burden in a PDX model. To our knowledge, this is the first report in which ovarian cancer PDX models

Downloaded from http://aacrjournals.org/mct/article-pdf/18/2/389/1861208/389.pdf by guest on 31 March 2023

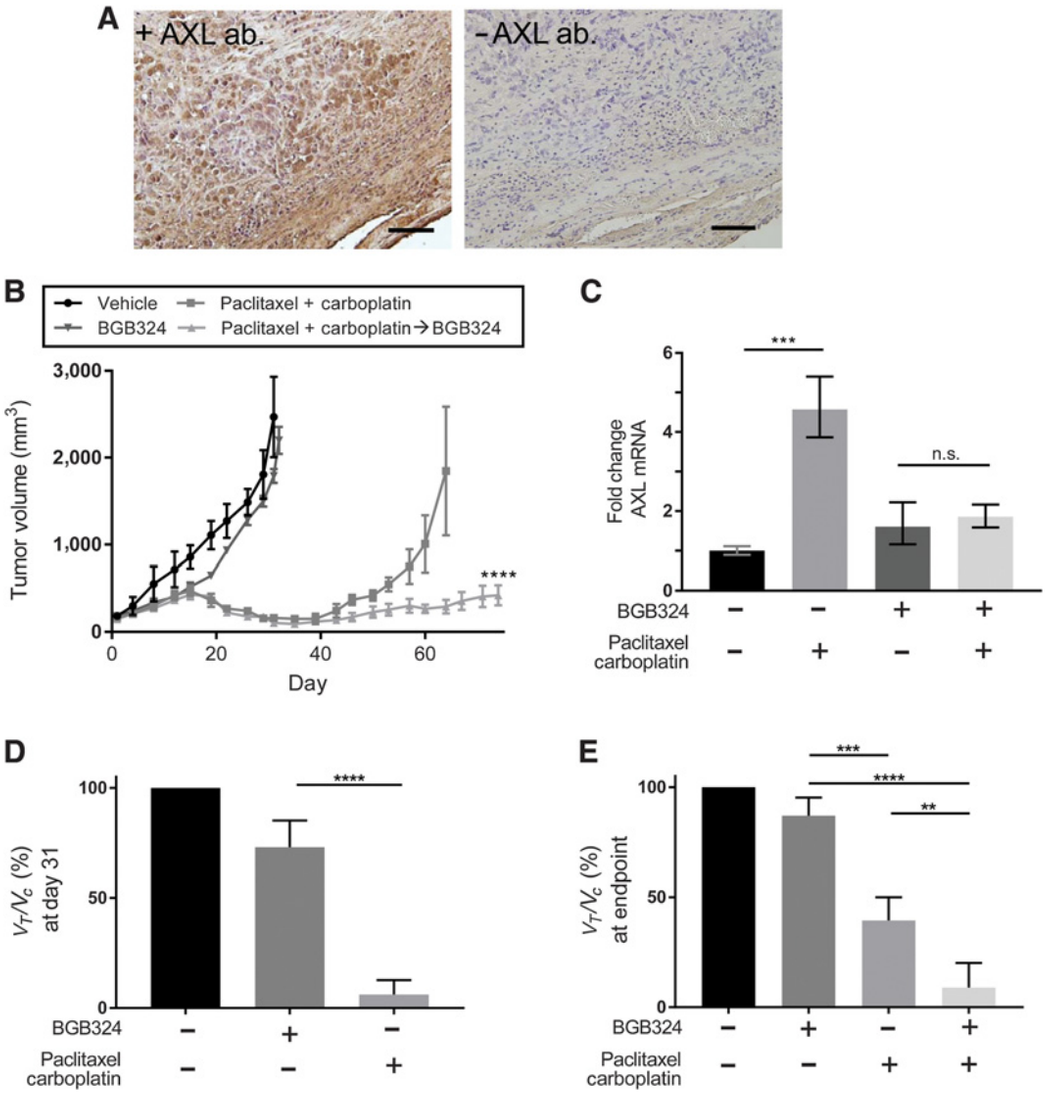

Figure 4.

AXL inhibition maintains chemoresponse in a chemoresistant PDX model. **A,** IHC analysis of the PDX tumor PB1 for AXL (left) with control negative for primary antibody (right). Scale bar, 100 mm. **B,** Volume of tumors over 74 days in mice engrafted with the PDX tumor PB1, and treated with vehicle, chemotherapy, BGB324, or chemotherapy then BGB324. Mean tumor volume and SE are plotted. ****, $P < 0.0001$ by one-way ANOVA. **C,** qPCR was performed on treated tumors and expression patterns of mRNA were assessed. Error bars indicate range of the fold change, and significance was calculated using SD of DDC_T. ***, $P < 0.001$. **C** and **D,** Quantitation of relative tumor proliferation rate ($V_{Treatment}/V_{Control}$) calculated by using the tumor volumes at day 31 (**D**) or endpoint (**E**) relative to tumor volumes at initial treatment administration. **, $P < 0.01$; ***, $P < 0.001$; ****, $P < 0.0001$.

are used to assess the efficacy of small-molecule inhibitors in combination with chemotherapy.

Several papers have examined relationships between AXL expression and chemoresistance. For example, increased AXL expression correlated with acute myelogenous leukemia progression on chemotherapy (52) and with resistance to antimitotic agents and platinum in several cancers (11, 15, 53). Additionally, AXL levels were correlated with resistance to platinum or antimitotic agents in lung cancer (28) and astrocytoma cell lines (53). Macleod found that AXL mRNA levels were 3-fold higher in platinum-resistant ovarian cancer cell lines than in platinum-sensitive cell lines (15). Corno and colleagues recently published that AXL expression correlated with aggressiveness of ovarian cancers, but they found that AXL inhibition did not increase chemosensitivity of the IGROV1-Pt1 cell line (17). In contrast, Kariolis and colleagues showed that AXL inhibition increased ovarian cancer response to the second-line/third-line chemotherapy drug doxorubicin (14). Kanlikilicer and colleagues demonstrate that AXL inhibition and paclitaxel treatment in an orthotopic animal model reduces tumor weight, but do not validate its significance when compared with AXL inhibition alone (8). Our data here and in our previous paper (13) indicate that inhibiting AXL increases ovarian and uterine cancer sensitivity to chemotherapy by increasing drug accumulation in the cells. Additional studies are required to assess if AXL inhibition improves accumulation of drugs besides paclitaxel and carboplatin. Moreover,

Downloaded from http://aacrjournals.org/mct/article-pdf/18/2/389/1861208/389.pdf by guest on 31 March 2023

our sequencing data suggest that this occurs via downregulation of genes encoding multidrug resistant proteins. Further investigation is required to determine the mechanism by which AXL regulates activity of these genes. Overall, our comprehensive inclusion of patient samples in TMA, cell lines, and *in vivo* models demonstrate that inhibition of AXL is a well-validated therapeutic option in platinum- or paclitaxel-resistant ovarian cancer.

Our data indicate that AXL expression can be used as an independent predictor of chemoresponse in ovarian cancer. To our knowledge, this is the first study to demonstrate that expression of AXL—or any molecular marker—can predict chemoresistance. We also performed RNA sequencing of pretreatment tumors to identify markers that were significantly different between patients who would (NED) and would not (AWD/DOD) respond to chemotherapy. More specifically, transcripts for AXL and two genes involved in drug accumulation, ABCA3 and ABCB9, were significantly higher in the AWD/DOD group than in the NED group, indicating that expression of these three genes might distinguish between tumors that will and will not respond to chemotherapy. Future work should be directed at determining whether any or all of these transcripts could be used as a prognostic factor or as a predictor of response to therapy in chemoresistant disease.

Disclosure of Potential Conflicts of Interest

I.S. Hagemann is a consultant/advisory board member for Change Healthcare and Bien-Willner Physicians Group and has been received for expert testimony. C.K. McCourt has received honoraria from the speakers bureau of Genentech and is a consultant/advisory board member for the same. P.H. Thaker reports receiving a commercial research grant from Merck, has received honoraria from the speakers bureau of Tesaro and Merck, has ownership interest (including stock, patents, etc.) in Celsion, and is a consultant/advisory board member for Tesaro and Celsion. No potential conflicts of interest were disclosed by the other authors.

Authors' Contributions

Conception and design: J.M. Quinn, D.G. Mutch, K.C. Fuh
Development of methodology: J.M. Quinn, M.M. Greenwade, M.L. Palisoul, K. Massad, L. Guo, I.S. Hagemann, K.C. Fuh
Acquisition of data (provided animals, acquired and managed patients, provided facilities, etc.): J.M. Quinn, M.M. Greenwade, M.L. Palisoul, G. Opara, L. Guo, I.S. Hagemann, A.R. Hagemann, C.K. McCourt, P.H. Thaker, M.A. Powell, D.G. Mutch, K.C. Fuh
Analysis and interpretation of data (e.g., statistical analysis, biostatistics, computational analysis): J.M. Quinn, M.M. Greenwade, G. Opara, P. Zhao, P.H. Thaker, D.G. Mutch, K.C. Fuh
Writing, review, and/or revision of the manuscript: J.M. Quinn, M.M. Greenwade, P.H. Thaker, D.G. Mutch, K.C. Fuh
Administrative, technical, or material support (i.e., reporting or organizing data, constructing databases): J.M. Quinn, M.M. Greenwade, M.L. Palisoul, G. Opara, K. Massad, H. Beck-Noia, D.G. Mutch
Study supervision: M.L. Palisoul, D.G. Mutch, K.C. Fuh

Acknowledgments

The authors thank Deborah Frank, PhD, for scientific editing of this manuscript and Thomas Walsh for assistance with constructing the tissue microarray (Washington University in St. Louis Breast Tissue Registry). Research reported in this publication was supported by NIH grant 2K12HD000849-28 (with co-funding from the American College of Obstetrics and Gynecologists, the Barnes Jewish Hospital Foundation, and the March of Dimes), Cancer Frontier Fund grants 8002-88 and 3794, and American Cancer Society grant IRG-58-010-59-3 (to K.C. Fuh).

The costs of publication of this article were defrayed in part by the payment of page charges. This article must therefore be hereby marked *advertisement* in accordance with 18 U.S.C. Section 1734 solely to indicate this fact.

Received May 17, 2018; revised July 11, 2018; accepted November 13, 2018; published first November 26, 2018.

References

1. Siegel RL, Miller KD, Jemal A. Cancer statistics, 2017. CA Cancer J Clin 2017;67:7–30.
2. Griffiths RW, Zee YK, Evans S, Mitchell CL, Kumaran GC, Welch RS, et al. Outcomes after multiple lines of chemotherapy for platinum-resistant epithelial cancers of the ovary, peritoneum, and fallopian tube. Int J Gynecol Cancer 2011;21:58–65.
3. Paccez JD, Duncan K, Vava A, Correa RG, Libermann TA, Parker MI, et al. Inactivation of GSK3beta and activation of NF-kappaB pathway via Axl represents an important mediator of tumorigenesis in esophageal squamous cell carcinoma. Mol Biol Cell 2015;26:821–31.
4. Wang C, Jin H, Wang N, Fan S, Wang Y, Zhang Y, et al. Gas6/Axl axis contributes to chemoresistance and metastasis in breast cancer through Akt/GSK-3beta/beta-catenin signaling. Theranostics 2016;6:1205–19.
5. Elkabets M, Pazarentzos E, Juric D, Sheng Q, Pelossof RA, Brook S, et al. AXL mediates resistance to PI3Kα inhibition by activating the EGFR/PKC/mTOR axis in head and neck and esophageal squamous cell carcinomas. Cancer Cell 2015;27:533–46.
6. Sun W, Fujimoto J, Tamaya T. Coexpression of Gas6/Axl in human ovarian cancers. Oncology 2004;66:450–7.
7. Antony J, Tan TZ, Kelly Z, Low J, Choolani M, Recchi C, et al. The GAS6-AXL signalling network is a mesenchymal (Mes) molecular subtype-specific therapeutic target for ovarian cancer. Sci Signal 2016;9:ra97.
8. Kanlikilicer P, Ozpolat B, Aslan B, Bayraktar R, Gurbuz N, Rodriguez-Aguayo C, et al. Therapeutic targeting of AXL receptor tyrosine kinase inhibits tumor growth and intraperitoneal metastasis in ovarian cancer models. Mol Ther Nucleic Acids 2017;9:251–62.
9. Byers LA, Diao L, Wang J, Saintigny P, Girard L, Peyton M, et al. An epithelial–mesenchymal transition gene signature predicts resistance to EGFR and PI3K inhibitors and identifies Axl as a therapeutic target for overcoming EGFR inhibitor resistance. Clin Cancer Res 2013;19:279–90.
10. Zhang Z, Lee JC, Lin L, Olivas V, Au V, LaFramboise T, et al. Activation of the AXL kinase causes resistance to EGFR-targeted therapy in lung cancer. Nat Genet 2012;44:852–60.
11. Wilson C, Ye X, Pham T, Lin E, Chan S, McNamara E, et al. AXL inhibition sensitizes mesenchymal cancer cells to antimitotic drugs. Cancer Res 2014;74:5878–90.
12. Gjerdrum C, Tiron C, Høiby T, Stefansson I, Haugen H, Sandal T, et al. Axl is an essential epithelial-to-mesenchymal transition-induced regulator of breast cancer metastasis and patient survival. Proc Natl Acad Sci U S A 2010;107:1124–9.
13. Palisoul ML, Quinn JM, Schepers E, Hagemann IS, Guo L, Reger K, et al. Inhibition of the receptor tyrosine kinase AXL restores paclitaxel chemosensitivity in uterine serous cancer. Mol Cancer Ther 2017;16:2881–91.
14. Kariolis MS, Miao YR, Diep A, Nash SE, Olcina MM, Jiang D, et al. Inhibition of the GAS6/AXL pathway augments the efficacy of chemotherapies. J Clin Invest 2017;127:183–98.
15. Macleod K, Mullen P, Sewell J, Rabiasz G, Lawrie S, Miller E, et al. Altered ErbB receptor signaling and gene expression in cisplatin-resistant ovarian cancer. Cancer Res 2005;65:6789–800.
16. Patch AM, Christie EL, Etemadmoghadam D, Garsed DW, George J, Fereday S, et al. Whole-genome characterization of chemoresistant ovarian cancer. Nature 2015;521:489–94.
17. Corno C, Gatti L, Arrighetti N, Carenini N, Zaffaroni N, Lanzi C, et al. Axl molecular targeting counteracts aggressiveness but not platinum resistance of ovarian carcinoma cells. Biochem Pharmacol 2017;136:40–50.

Downloaded from http://aacrjournals.org/mct/article-pdf/18/2/389/1861208/389.pdf by guest on 31 March 2023

18. Rankin EB, Fuh KC, Taylor TE, Krieg AJ, Musser M, Yuan J, et al. AXL is an essential factor and therapeutic target for metastatic ovarian cancer. Cancer Res 2010;70:7570–9.
19. Domcke S, Sinha R, Levine DA, Sander C, Schultz N. Evaluating cell lines as tumour models by comparison of genomic profiles. Nat Commun 2013; 4:2126.
20. Moisan F, Francisco EB, Brozovic A, Duran GE, Wang YC, Chaturvedi S, et al. Enhancement of paclitaxel and carboplatin therapies by CCL2 blockade in ovarian cancers. Mol Oncol 2014;8:1231–9.
21. Holland SJ, Pan A, Franci C, Hu Y, Chang B, Li W, et al. R428, a selective small molecule inhibitor of Axl kinase, blocks tumor spread and prolongs survival in models of metastatic breast cancer. Cancer Res 2010;70:1544–54.
22. Heinrich MC, Griffith DJ, Druker BJ, Wait CL, Ott KA, Zigler AJ. Inhibition of c-kit receptor tyrosine kinase activity by STI 571, a selective tyrosine kinase inhibitor. Blood 2000;96:925–32.
23. Counter CM, Hahn WC, Wei W, Caddle SD, Beijersbergen RL, Lansdorp PM, et al. Dissociation among in vitro telomerase activity, telomere maintenance, and cellular immortalization. Proc Natl Acad Sci U S A 1998;95:14723–8.
24. Rankin EB, Fuh KC, Castellini L, Viswanathan K, Finger EC, Diep AN, et al. Direct regulation of GAS6/AXL signaling by HIF promotes renal metastasis through SRC and MET. Proc Natl Acad Sci U S A 2014;111:13373–8.
25. Pinzon-Daza ML, Cuellar-Saenz Y, Nualart F, Ondo-Mendez A, Del Riesgo L, Castillo-Rivera F, et al. Oxidative stress promotes doxorubicin-induced Pgp and BCRP expression in colon cancer cells under hypoxic conditions. J Cell Biochem 2017;118:1868–78.
26. Kuan C-T, Wakiya K, Herndon JE 2nd, Lipp ES, Pegram CN, Riggins GJ, et al. MRP3: a molecular target for human glioblastoma multiforme immunotherapy. BMC Cancer, 2010;10:468.
27. Morrison JG, White P, McDougall S, Firth JW, Woolfrey SG, Graham MA, et al. Validation of a highly sensitive ICP-MS method for the determination of platinum in biofluids: application to clinical pharmacokinetic studies with oxaliplatin. J Pharm Biomed Anal 2000;24:1–10.
28. Linger RM, Cohen RA, Cummings CT, Sather S, Migdall-Wilson J, Middleton DH, et al. Mer or Axl receptor tyrosine kinase inhibition promotes apoptosis, blocks growth and enhances chemosensitivity of human non–small cell lung cancer. Oncogene 2013;32:3420–31.
29. Fleuren ED, Hillebrandt-Roeffen MH, Flucke UE, Te Loo DM, Boerman OC, van der Graaf WT, et al. The role of AXL and the in vitro activity of the receptor tyrosine kinase inhibitor BGB324 in Ewing sarcoma. Oncotarget 2014;5:12753–68.
30. Lin JZ, Wang ZJ, De W, Zheng M, Xu WZ, Wu HF, et al. Targeting AXL overcomes resistance to docetaxel therapy in advanced prostate cancer. Oncotarget 2017;8:41064–77.
31. Del Pozo Martin Y, Park D, Ramachandran A, Ombrato L, Calvo F, Chakravarty P, et al. Mesenchymal cancer cell-stroma crosstalk promotes niche activation, epithelial reversion, and metastatic colonization. Cell Rep 2015;13:2456–69.
32. Aberuyi N, Rahgozar S, Khosravi Dehaghi Z, Moafi A, Masotti A, Paolini A. The translational expression of ABCA2 and ABCA3 is a strong prognostic biomarker for multidrug resistance in pediatric acute lymphoblastic leukemia. Onco Targets Ther 2017;10:3373–80.
33. Dong Z, Zhong Z, Yang L, Wang S, Gong Z. MicroRNA-31 inhibits cisplatin-induced apoptosis in non–small cell lung cancer cells by regulating the drug transporter ABCB9. Cancer Lett 2014;343:249–57.
34. Gong JP, Yang L, Tang JW, Sun P, Hu Q, Qin JW, et al. Overexpression of microRNA-24 increases the sensitivity to paclitaxel in drug-resistant breast carcinoma cell lines via targeting ABCB9. Oncol Lett 2016;12:3905–11.
35. Oien DB, Garay T, Eckstein S, Chien J. Cisplatin and pemetrexed activate AXL and AXL inhibitor BGB324 enhances mesothelioma cell death from chemotherapy. Front Pharmacol 2017;8:970.
36. Stockler MR, Hilpert F, Friedlander M, King MT, Wenzel L, Lee CK, et al. Patient-reported outcome results from the open-label phase III AURELIA trial evaluating bevacizumab-containing therapy for platinum-resistant ovarian cancer. J Clin Oncol 2014;32:1309–16.
37. Coleman RL, Monk BJ, Sood AK, Herzog TJ. Latest research and treatment of advanced-stage epithelial ovarian cancer. Nat Rev Clin Oncol 2013; 10:211–24.
38. Xu Y, Miao C, Jin C, Qiu C, Li Y, Sun X, et al. SUSD2 promotes cancer metastasis and confers cisplatin resistance in high grade serous ovarian cancer. Exp Cell Res 2018;363:160–70.
39. Leung CS, Yeung TL, Yip KP, Wong KK, Ho SY, Mangala LS, et al. Cancer-associated fibroblasts regulate endothelial adhesion protein LPP to promote ovarian cancer chemoresistance. J Clin Invest 2018;128: 589–606.
40. Raghavan S, Mehta P, Ward MR, Bregenzer ME, Fleck EMA, Tan L, et al. Personalized medicine-based approach to model patterns of chemoresistance and tumor recurrence using ovarian cancer stem cell spheroids. Clin Cancer Res 2017;23:6934–45.
41. Somasagara RR, Spencer SM, Tripathi K, Clark DW, Mani C, Madeira da Silva L, et al. RAD6 promotes DNA repair and stem cell signaling in ovarian cancer and is a promising therapeutic target to prevent and treat acquired chemoresistance. Oncogene 2017;36:6680–90.
42. Liu J, Agopiantz M, Poupon J, Wu Z, Just PA, Borghese B, et al. Neurotensin receptor 1 antagonist SR48692 improves response to carboplatin by enhancing apoptosis and inhibiting drug efflux in ovarian cancer. Clin Cancer Res 2017;23:6516–28.
43. Momeny M, Zarrinrad G, Moghaddaskho F, Poursheikhani A, Sankanian G, Zaghal A, et al. Dacomitinib, a pan-inhibitor of ErbB receptors, suppresses growth and invasive capacity of chemoresistant ovarian carcinoma cells. Sci Rep 2017;7:4204.
44. Chakraborty PK, Mustafi SB, Xiong X, Dwivedi SKD, Nesin V, Saha S, et al. MICU1 drives glycolysis and chemoresistance in ovarian cancer. Nat Commun 2017;8:14634.
45. Roberts CM, Tran MA, Pitruzzello MC, Wen W, Loeza J, Dellinger TH, et al. TWIST1 drives cisplatin resistance and cell survival in an ovarian cancer model, via upregulation of GAS6, L1CAM, and Akt signalling. Sci Rep 2016;6:37652.
46. Stronach EA, Cunnea P, Turner C, Guney T, Aiyappa R, Jeyapalan S, et al. The role of interleukin-8 (IL-8) and IL-8 receptors in platinum response in high-grade serous ovarian carcinoma. Oncotarget 2015; 6:31593–603.
47. Chiu WT, Huang YF, Tsai HY, Chen CC, Chang CH, Huang SC, et al. FOXM1 confers to epithelial–mesenchymal transition, stemness and chemoresistance in epithelial ovarian carcinoma cells. Oncotarget 2015; 6:2349–65.
48. Kang Y, Nagaraja AS, Armaiz-Pena GN, Dorniak PL, Hu W, Rupaimoole R, et al. Adrenergic stimulation of DUSP1 impairs chemotherapy response in ovarian cancer. Clin Cancer Res 2016;22:1713–24.
49. Ricci JW, Lovato DM, Severns V, Sklar LA, Larson RS. Novel ABCG2 antagonists reverse topotecan-mediated chemotherapeutic resistance in ovarian carcinoma xenografts. Mol Cancer Ther 2016;15: 2853–62.
50. Musa F, Alard A, David-West G, Curtin JP, Blank SV, Schneider RJ. Dual mTORC1/2 inhibition as a novel strategy for the re-sensitization and treatment of platinum-resistant ovarian cancer. Mol Cancer Ther 2016; 15:1557–67.
51. Wilson AJ, Liu AY, Roland J, Adebayo OB, Fletcher SA, Slaughter JC, et al. TR3 modulates platinum resistance in ovarian cancer. Cancer Res 2013; 73:4758–69.
52. Loges S. A first-in-patient phase I study of BGB324, a selective Axl kinase inhibitor in patients with refractory/relapsed AML and high-risk MDS. J Clin Oncol 2016;34:2561.
53. Keating AK, Kim GK, Jones AE, Donson AM, Ware K, Mulcahy JM, et al. Inhibition of Mer and Axl receptor tyrosine kinases in astrocytoma cells leads to increased apoptosis and improved chemosensitivity. Mol Cancer Ther 2010;9:1298–307.

Downloaded from http://aacrjournals.org/mct/article-pdf/18/2/389/1861208/389.pdf by guest on 31 March 2023